Article **ECORFAN Journal-Democratic Republic of Congo**
December 2018 Vol.4 No.7 27-37

Optical and photocatalytic properties of TiO_2/ZnO composites

Propiedades ópticas y fotocatalíticas de los compuestos de TiO2 / ZnO

TIRADO-GUERRA, Salvador*† & VALENZUELA-ZAPATA, Miguel

Escuela Superior de Física y Matemáticas del IPN, Edificio 9, U.P. "A.L.M." San Pedro Zacatenco, C.P. 07738, CDMEX, México. Laboratorio de Catálisis y Materiales, ESIQIE del IPN, Edificio 8, U.P. "A.L.M.", San Pedro Zacatenco, C.P. 07738, CDMEX, México.

ID 1st Author: *Salvador, Tirado-Guerra/* **ORC ID:** 000-0001-9799-9963

ID 1st Coauthor: *Miguel, Valenzuela-Zapata/* **ORC ID:** 0000-0002-8430-062X

Received July 11, 2018; Accepted November 16, 2018

Abstract

TiO_2/ZnO composites were synthesized in thin film by sol-gel route and repeated immersion and grown on soda-lime substrates. The composites were studied and characterized with various experimental techniques. TiO_2 layers were grown to five layers thick and on these several layers of ZnO were grown, forming the TiO_2/ZnO composites. The morphology and chemical composition was evaluated by SEM and EDS, phases were determined by XRD and Raman, the topography was recorded by AFM, with UV-Vis spectroscopy the optical properties, and the ionic state of components of the composition were evaluated by XPS. Porous films composed of Ti, Zn and O were identified, the TiO_2/ZnO films showed a wurtzite hexagonal structure with a crystal size of 18.0 nm; untransparent films and an *Eg* around 3.00 eV resulted. Ion states and binding energies of Ti, Zn, O and C were determined. The catalytic and photoluminescent activity of the TiO_2/ZnO composites were recorded, where MO degradation and emission spectra in the UV and visible region, were obtained. From the synthesized composites and the properties obtained from the study, as catalysts, as well as radiation detectors, were obtained in the UV-Vis range.

TiO_2/ZnO, Photodegradation, Photoluminescence

Resumen

Se sintetizaron compositos TiO_2/ZnO en película delgada por ruta sol-gel e inmersión repetida y creciéndose sobre sustratos sodo-cálcicos. Los compositos se estudiaron y caracterizaron con diversas técnicas experimentales. Se crecieron camas de TiO_2 a cinco capas de espesor y sobre éstas se crecieron diversas capas de ZnO, formando los compositos TiO_2/ZnO. La morfología y composición química se evaluó por MEB y EDS, se determinaron fases por DRX y Raman, se registró la topografía por MFA, con espectroscopia UV-Vis se evaluaron propiedades ópticas y el estado iónico de componentes del composito por XPS. Películas porosas compuestas de Ti, Zn y O se identificaron, las películas TiO_2/ZnO presentaron una estructura hexagonal wurtzita con un tamaño de cristal de 18.0 nm; películas poco transparentes y un *Eg* alrededor de 3.00 eV resultaron. Estados iónicos y energías de enlace de Ti, Zn, O y C se determinaron. Se registró la actividad catalítica y fotoluminiscente de los compuestos de TiO_2/ZnO, donde se obtuvieron la degradación de MO y los espectros de emisión en la región UV y visible. De los compositos sintetizados y las propiedades obtenidas del estudio, se obtuvieron catalizadores, así como detectores de radiación, en el rango del UV-Vis.

TiO_2/ZnO, Fotodegradación, Fotoluminiscencia

Citation: TIRADO-GUERRA, Salvador & VALENZUELA-ZAPATA, Miguel. Optical and photocatalytic properties of TiO_2/ZnO composites. ECORFAN Journal-Democratic Republic of Congo 2018, 4-7: 27-37

* Correspondence to Author (email: tirado@esfm.ipn.mx)
† Researcher contributing first author.

Article **ECORFAN Journal-Democratic Republic of Congo**
December 2018 Vol.4 No.7 27-37

Introduction

The most important semiconductor oxide is titanium dioxide (TiO_2) for its multiple applications in fields of interest in the industry, in coatings, in photocatalysis, among others (Yu, J., et al., (2000), Chae, Y.K., et al., (2013), Hermann, J.M., (1995), Hermann, J.M., et al., (1999)). In photocatalysis, the phase of interest is the anatase of TiO_2, an indirect band semiconductor with bandwidth around 3.2 eV, phase related to low temperatures, low density and is preferred, to be applied in photodegradation of polluting substances in water and the environment (Yu, J., et al., (2000), Chae, Y.K., et al., (2013), Ochoa, Y., et al., (2009), Nada, A., et. al., (2010)).

The anatase TiO_2 phase, in powders or in films on suitable substrates, is obtained with nanotube structures or other types (Ochoa, Y., et al., (2009), Nada, A., et al., (2010), Luna, A.L., et al., (2016), Giannakopoulou T., et al., (2014)). On physical methods, chemical methods are preferred, which offer several advantages. We use the sol-gel chemical route and repeated immersion to grow thin films of TiO_2, where several experimental parameters are controlled to obtain high quality films and good physical and chemical properties.

The anatase phase TiO_2 films have high adhesion to substrates of soda-calcic glass and are prepared with precursors of metal alkoxides in solutions, films with large specific area, morphology and structure, allowing to putting them in contact with various interfaces, aqueous or gaseous media, with the which can be reacting and as a consequence can be applied in heterogeneous catalysis. TiO_2 with bandwidth around 3.2 eV, to apply it in a reaction, it must be irradiated, in principle with sunlight, so little response is expected due to the low proportion of UV radiation in the solar spectrum (λ <372 nm) (Luna, A.L., et al., (2016), Castrejón-Sánchez, V.H., et al., (2014)) and since the catalyst to be useful must respond to being irradiated, generating pairs of charges (e^- and h^+), transferring charges from the valence band (VB) to the conduction band (CB), which can be used in possible oxide-reduction reactions (Luna, A.L., et al., (2016), Castrejón-Sánchez, V.H., et al., (2014)).

When the bandwidth of a catalyst, TiO_2 or ZnO, is an obstacle to be applied as such, and thus be able to degrade a tracer substance, the optical properties of the semiconductor can be improved, by impurifying the package or by superficially incorporating metals such as Cu, Ag, among others, with which it is possible to modify the properties of the semiconductor (Nada, A., et al., (2010)); also, synthesizing composite systems such as CuO-TiO_2 and testing its catalytic activity when degrading gallic acid (Luna, A.L., et al., (2016)). In a recent work, Luna, A.L., et al., (2017) report TiO_2 systems where they make bimetallic modifications, that is, they incorporate Ni and Pd to TiO_2 to improve the absorption of light, which is of interest.

Chemical reactions can be induced by the absorption of UV light by a catalyst, since photoelectrons and holes are generated, there is a separation of charges, promoting the electron to the conduction band, which can migrate to the surface of the interface between TiO_2 semiconductors and ZnO, where charge carriers can be exchanged or a reaction with the environment can be made. In addition, if there is moisture or water, it can be ionized generating hydroxyl radicals (OH^-) that are very reactive and can participate in oxide-reduction reactions, where contaminating molecules can be degraded or mineralized (Chae, Y.K., et al., (2013), Hermann, J.M., et al., (1999)). O_2 molecular oxygen can also participate by trapping a photoelectron e^- to form a defect-oxygen state, whose energy falls in the forbidden band of the semiconductor, thus having a radical super-oxide (O^{2-}) that can participate in reactions and/or in charges transitions between interfaces (Chae, Y.K., et al., (2013), Yu, J., et al., (2000)).

Thus, continuing with the composites, and using TiO_2 films as a substrate grown on glass, several layers of ZnO are deposited to generate the TiO_2/ZnO composites, of interest in this study. In addition to being characterized by several techniques, both optical and photocatalytic properties are evaluated by decomposing an aqueous solution of methyl orange (MO) at 14 ppm, in addition to evaluating the photo-luminescent response of the composites, when they are irradiated with UV light.

ISSN-On line: 2414-4924
ECORFAN® All rights reserved.

The work is presented in the order: introduction-justification, experimental method, synthesis and preparation of films, film growth, characterization techniques, results, XRD, SEM and EDS, AFM, UV-Vis, X-rays photoelectron spectroscopy (XPS), photocatalysis and photoluminescence, conclusions, acknowledgments and references.

Methodology experimental

Synthesis and films preparation

Thin TiO_2 films were prepared from a 0.2 M sol of the titanium oxy acetylacetonate precursor salt in 2-methoxyethanol and monoethanolamine, with a 1: 1 ratio of the salt to the latter. Under constant magnetic stirring for 2 h and at room temperature, a clear solution with a pH of 7 was obtained. Thin films of TiO_2 were prepared at a thickness of five dives on soda-lime glass substrates. Part of the films were surface modified with layers of zinc oxide films, prepared from a sol of zinc acetate in 0.4 M ethanol, with a pH of 6. Thus TiO_2/ZnO composites in thin films, systems that are characterized and studied. The chemical technique of sol-gel and repeated immersion, technique implemented in the laboratory, were used (Maldonado A., et al., (2010)).

Film growth

The growth of the films on previously prepared glass substrates, was carried out by repeated immersion of the substrate and at room temperature, with a process implemented and controlled by a PC. For each immersion and extraction of the substrate from the sol, drying is carried out for 10 min at a temperature of 250 °C of the oven with air. The process is repeated until the thickness required for the film is achieved. A heat treatment is given at 300 °C for 1 hour and the films stabilize and improve their properties. A Thermoline Furnace 6000 furnace was used. The TiO_2 films (87 nm) are grown and then modified with ZnO layers (133 nm) and thus the TiO_2/ZnO composites (TZi, with i = 0, 1, 3 and 5 samples) are obtained and studied.

Characterizations

The XRD diffraction patterns of the TiO_2/ZnO films were recorded with θ-2θ symmetric geometry in a Panalytical X'pert PRO diffractometer, using the *Kα* line of *Cu* (λ = 0.15406 nm).

The Raman spectra were recorded on a LabRam spectrometer, model HR 800 and Horiba Jobin Yvon brand (400-4000 cm^{-1}). The SEM micrographs and EDS of TZi thin film composites are recorded in a JSM 7800-JEOL 4527 electronic microscope. The topography of the TZi films was recorded in a PARK AutoProbe Equipment microscope (Veeco) with a 10 μm silicon tip in the intermittent mode. The optical properties and degradation in a GBC spectrometer model Cintra 20. The ionization states of the Ti, O and Zn components of the films were determined by XPS photoelectron spectroscopy (Thermo Scientific K Alfa, Double Source Mg and Al). The emission spectra of the samples were recorded in a Shimadzu RF-5301PC spectrofluorophotometer.

Results

X-ray diffraction

The X-ray diffraction (XRD) patterns of the TZi films were polycrystalline (Graph 1) for 3 and 5 layers of ZnO and peaks at: 31,684°, 34,281°, 36,290°, 49,373°, 57,213°, wide peak at 62,162° , 68,630°, 78,822° (JCPDS 036-1451 card) (wurtzite structure of ZnO). The phases of TiO_2 was not identified. The preferential peak in the spectrum at 34,286° is associated to the plane (0 0 2) and from that the crystal size *D* is estimated according to the Debye-Scherrer ratio, $D = 0.9\lambda/\beta cos\theta$, resulting in a *D* of 18-20 nm range. The anatase (JCPDS 021-1272) and rutile phases (JCPDS 021-1276) are not defined in this case for TiO_2.

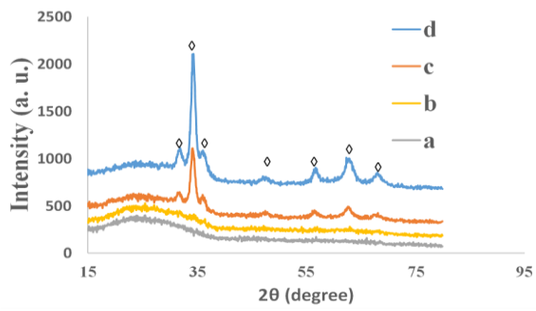

Graphic 1 Diffragrams show a) TZ0, b) TZ1, c) TZ3 and d) TZ5 samples

ECORFAN® All rights reserved.

Raman spectroscopy

From the recorded spectra at room temperature (Graph 2) the modes: 164, 243.4, 276, 326, 356, 397, 437, 486, 514, values in cm^{-1}, were recorded. The identification of the recorded data: 326 with 340 (E2 (HL)), 356 with 380 A1 (T), 397 with 408 E1 (T), 437 with 437 (E2 (H)), values in cm^{-1}, were proposed (Ramirez Ortega D., et al., (2014)); for our ZnO films the frequencies registered in 164 and 767 cm^{-1} can be related to intermediate byproducts such as ($ZnO(OH)_2$) (López, R., et al., (2011)). Such possible assignments identify the wurtzite hexagonal phase of prepared ZnO films, as was did with XRD. Others assignments for ZnO films are given (Damen, T.C., et al., (1966), Pérez Taborda, J.A., et al., (2008)). Using Raman technique to define the phases of ZnO is required to be prepared at high temperatures and not only to the environment. On the other hand, the identification of phonons in a given system (wires, spheres, etc.) requires theoretical calculations (Lara A., del Angel, Master Thesis. (2014)).

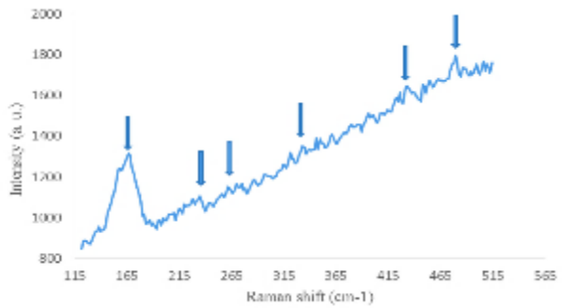

Graphic 2 Raman spectrum representative of the TZi composites

Scanning electron miscroscopy

Scanning micrographs of the TiO_2/ZnO samples, were recorded (not shown) at diffferent magnifications, especially of TZ0 and those of TZ1 with a ZnO layer, both resulted with fine grains and at higher magnification show their porosity and morphology and the presence of ZnO nanoparticles in the second case.

The analysis by EDS (Table not shown) of the TZi films, both pure and that with a deposit of ZnO, shows the presence of oxygen and titanium in the pure and also zinc in the case of sample with one ZnO layer, respectively.

Atomic force microscopy

The roughness parameters Rq, Ra and Rmax for an area 2 μm x 2 μm scanned (Table I), the parameters were of the order of nanometers, so the films are of low roughness. The micrographs (Figures 1 and 2) represent the topographic characteristics of the TZi sol-gel composites, and they show interesting surface granular formations and pores that give a contrast and a homogeneous grain size distribution in the first case (Graph 3), while a non-symmetric distribution is presented in other samples. The uniform grain size distribution in Graph 3 resulted in around 17.7 nm.

Samples	Rq (nm)	Ra (nm)	Rmax (nm)
TZ0	0.209	0.166	1.710
TZ1	0.245	0.186	2.120
TZ3	17.30	14.70	104.00

Table 1 Roughness parameters for TZ0, TZ1 and TZ3 samples

The AFM topography in Figures 1 and 2 correspond to a scale of 2 μm x 2 μm, from which the roughness parameters for the TZi samples, both TZ0 and TZ1 samples; such parameters are shown in Table 1 (TZ0, TZ1, TZ3), were evaluated. Graph 3 shows the average and uniform grain size distribution for the TZ0 sample.

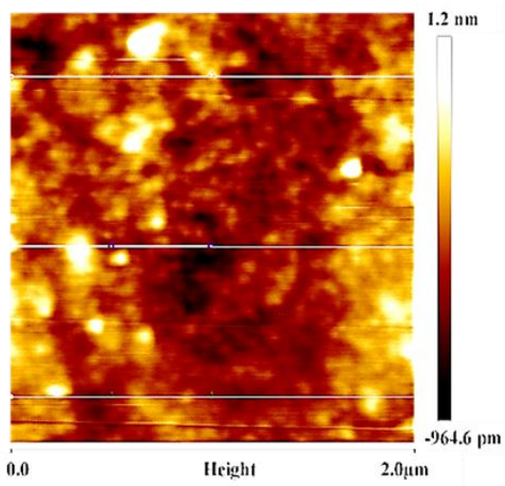

Figure 1 AFM image representative of the TZ0 sample of the series TZi under study

ECORFAN® All rights reserved.

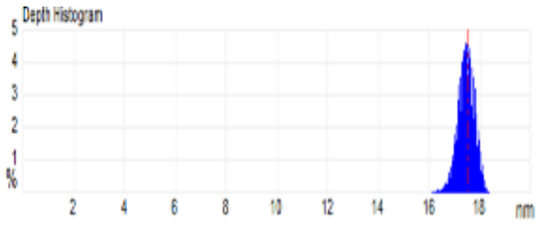

Graphic 3 Grain size distribution of the pure TZ0 sample

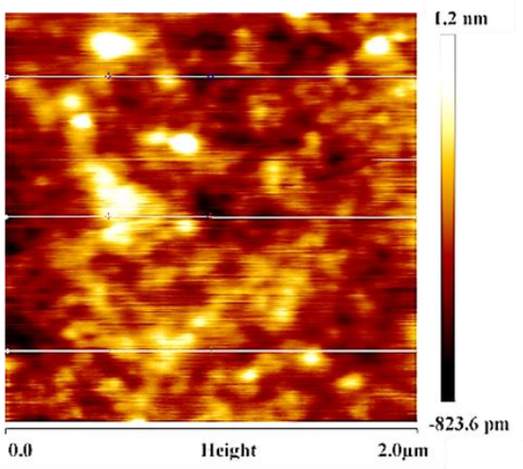

Figure 2 AFM image of film TZ1 with a ZnO layer of the series

UV-Vis spectroscopy

The spectra of the TZi samples (Graph 4) were semitransparent with absorption board at 375, 373, 343 and 399 nm, for zero, one, three and five layers of ZnO, respectively, although no congruent trend was observed; the spectra show interference effects that come from the TiO_2 growth process, although with a disorder for the first deposit of ZnO, but for three and five layers, the structural order of growth of the ZnO films appears, being clearer with five layers of ZnO. From the interference of the patterns, important parameters that characterize the films were evaluated, such as film thickness (Jongnavakit P., et al., (2012), Martínez A.I., et al., (2005)).

As the transmittance T% is recorded in the spectra and the relation of this with the reflectance (R%), the ratio $R\% = (1-T\%)/(1 + T\%)$ and that of the refractive index $n = (1 + R_{1/2})/(1-R_{1/2})$, the behavior of the index for the film is determined (Jongnavakit P., et al., (2012), Martínez A.I., et al., (2005)). The band gap *Eg* estimated, was around 3.00 eV for the pure sample and a slightly lower value is obtained for the sample with a layer of ZnO.

The Kubelka-Munk relation (Liu F., et al., (2016)) is used to estimate the band gap of the TiO_2/ZnO complex semiconductor, the graph of $(\alpha hv)^2 = A(hv - Eg)$ when extrapolated to the energy axis of the photon hv (with α zero) (Jongnavakit P., et al., (2012), Martínez A.I., et al., (2005), Pérez-Alvarez J., et al. , (2007)), with A a constant that depends on the material and α is the absorption coefficient given by the relation $\alpha(\lambda) = ln(1/T)/d$, with d the thickness of the film. There is no consistent trend in the evaluations.

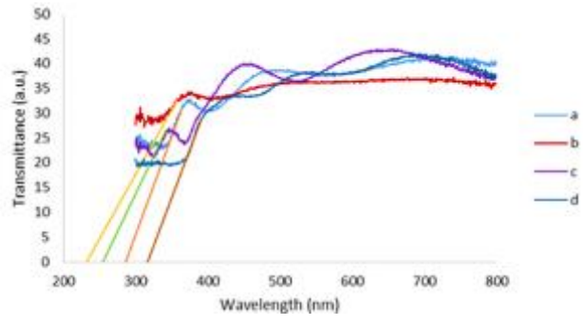

Graphic 4 UV-Vis spectra of TZi samples and slopes with Eg: TZ0 a) 2.86 eV, TZ1 b) 2.33 eV, TZ3 c) 2.55 eV and TZ5 d) 3.17 eV

XPS spectroscopy

The general spectrum of the TiO_2/ZnO composite system was recorded, which is presented in Graph 5, where the presence of the Zn2p and Ti2p orbitals, as well as oxygen and carbon, among others, are observed. The position of the bond energies of the spin-orbital Ti2p ($2p_{3/2}$ and $2p_{1/2}$) for Ti^{4+} were recorded at 458.78 eV and 464.88 eV, respectively, with a $\Delta E = 6.1$ eV (Graph 6); also it is found the 472.28 eV value, possibly associated with Ti^{3+} which gives non-stoichiometric characteristics of the surface in the films (Fusi M., et al., (2011)). The Zn2p orbitals were recorded at: 1020.98 eV ($2p_{3/2}$) and 1044.88 eV ($2p_{1/2}$) with a $\Delta E = 23.9$ eV (Graph 7). The high-resolution spectra of the O1s and of C1s orbitals were recorded, and discussed in detail below.

ECORFAN® All rights reserved.

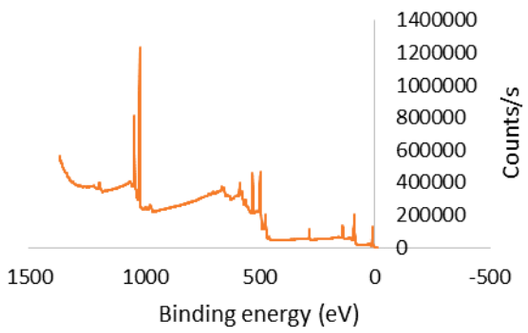

Graphic 5 General XPS spectrum showing the presence of TiO_2/ZnO composites

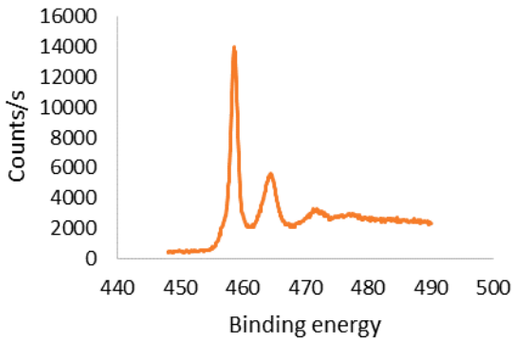

Graphic 6 Orbitals of Ti^{4+}, in 458.78 eV ($2p_{3/2}$) and in 464.88 eV ($2p_{1/2}$) with ΔE = 6.1 eV

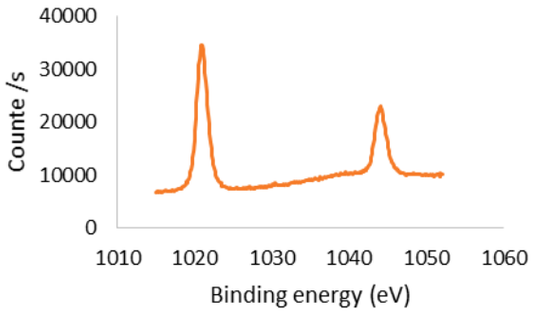

Graphic 7 Orbital Zn2p of zinc in 1020.98 eV ($2p_{3/2}$) and 1044.88 eV ($2p_{1/2}$) with ΔE = 23.9 eV

Graph 8 shows the high resolution O1s orbital spectrum of the oxygen in TiO_2/ZnO samples with the respective species according to the CasaXPS program. Measured data for the maximum were: 530.18 eV (TZ0), 529.68 eV (TZ3) and 530.18 eV (TZ5), the intensity is different in each case, and from deconvolution of spectra, were found essentially two components: the decomposition of the O1s orbital for the main component were: 530.23, 529.59 and 531. 84 eV in each case, and for the second component were: 531.03, 530.65 and 531.84 eV, respectively.

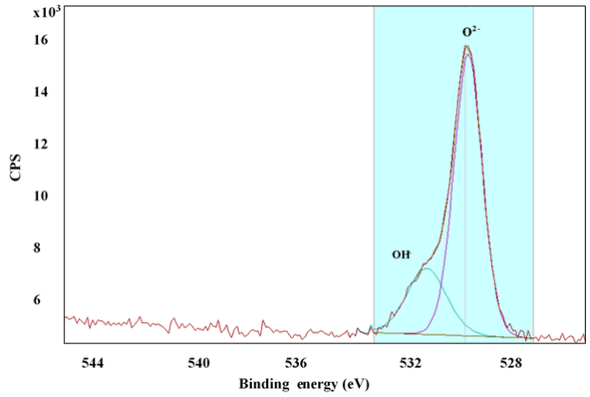

Graphic 8 Analysis of the O1s orbital for the surface oxygen of the ZnO film

The main adjustment component can be associated to O^{2-} in the network of the formula ZnO or to the bond in TiO_2 (Fusi, M., et al., (2011), Liu, F., et al., (2016) , Yu, J., et al., (2010)); the peak at 531.84 eV of the adjustment of the second component can be associated with hydroxyl OH^- and possible C-C or C = C bonds, since there are no differences detectable in energy (Liu F., et al., (2016), Fusi M ., et al. (2011), Yu J., et al., (2010)), that with temperature could be defined (Liu, F., et al., (2016); due to the registered signal and the adjustment applied, no signal was found that could be associated with H_2O molecules or other compounds such as Ti_2O_3 (Yu, J., et al., (2010)).

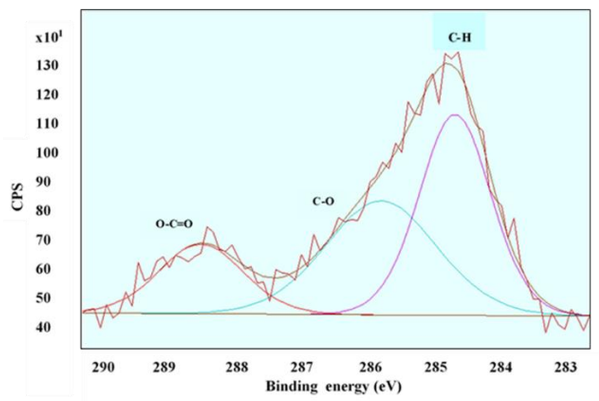

Graphic 9 Analysis of the C1s orbital for the surface carbon in the ZnO film

The type of spectrum recorded for the carbon C1s orbital is shown (Graph 9). According to the CasaXPS program and with a line shape GL(30) (Gauss-Lorentz) and records in different points from the respective sample, for the pure sample of TiO_2/ZnO (TZ0), the adjustment program yields three components or peaks with the 284.78, 286.28 and 288.08 eV values.

ISSN-On line: 2414-4924
ECORFAN® All rights reserved.

For samples with three and five layers of ZnO, the positions change little, both in intensity and in the average width, so it can be said that there are species with different concentrations and intensities (Liu, F., et al., (2016), Yu, J., et al., (2010)). We have thus for the C1s orbital the possible groups of C-C or C-H bonds (284.78 eV), C-O (286.28 eV) and the O-C = O (288.08 eV), which would indicate different groups of organic residues on ZnO particles; the different possible signals of the adjustment come from conditions such as contact with air during the process and the heat treatment given to the samples (Liu, F., et al., (2016), Fusi, M., et al. 2011), Yu, J., et al., (2010)). All analyzed XPS spectra are referred to the C1s at 284.78 eV position of the main peak.

Catalytic activity

The photodegradation of MO at 14 ppm with TiO_2/ZnO systems was carried out in a rectangular reactor with 8 blue lamps (G8T5) with an irradiance of 7.0x200 candles/pie^2 (visible) and 2.2x200 candles/pie^2 (UVA). Graph 10 shows the degradation of MO by the pure TZ0 sample every 15 min up to 2 hours. Graph 11 shows the MO degradation of the maximum at 504 nm by the TZi samples (TZ0, TZ1, TZ3 and TZ5 samples). The response in general is low.

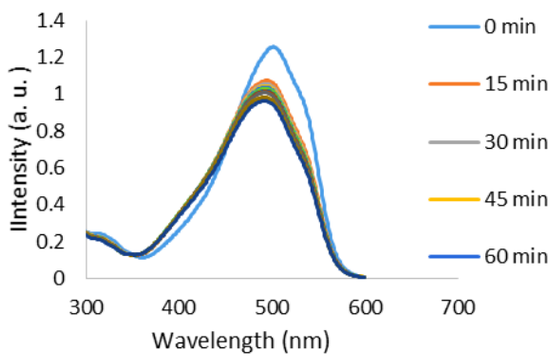

Graphic 10 First degradation cycle of MO for every 15 min up to 2 hours, of the pure TZ0 sample

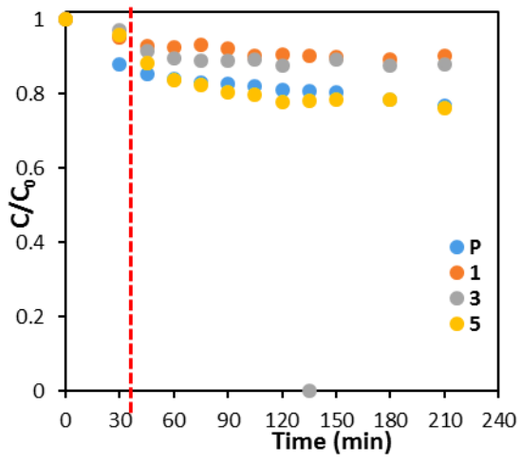

Graphic 11 Degradation of MO for every 15 min up to 2 hours, of the maximum 504 nm of each sample of the TZi series

Graphs 10 and 11 show the process of MO degradation by the TZi samples of the band around 504 nm, by irradiating the aqueous film-solution every 15 min, for a period of 2 hours.

The degradation speed of MO given by the decrease of the intensity of the indicated band, is proportional to the C concentration of the MO, according to the kinetic equation of pseudo first order, given by $C = C_0\ e^{-kt}$, with k pseudo constant of the reaction and t is the irradiation time of the study system. From the recorded data of the MO degradation process by the samples and the adjustment of the relationship between the C_0 and C concentrations for the various times t, the reaction constants of each system were evaluated, resulting in the k of the pure sample TiO_2/ZnO (TZ0) slightly higher than what is evaluated for the film TZ1 with a ZnO catalyst layer, a better response was to be expected. By increasing the catalyst should have a better response. According to Figures 1 and 2, and the roughness parameters given in Table 1, those corresponding to the composite with a ZnO layer were relatively better, however, there is no better response in the catalytic activity. In principle, roughness, surface area and grain size should play an important role in catalytic activity.

ISSN-On line: 2414-4924
ECORFAN® All rights reserved.

The heat treatment in the film with one or more layers of ZnO, allows the grain size to grow and the number of grain boundaries to be reduced, which greatly affects the charge transfer activity between the interfaces of the composite, decreasing consequently the catalytic activity of the films; the stress states, surface defects, the quantity of hydroxyl OH^-, as well as oxygen vacancies and the specific surface area of the composite, also participate in a very important way (Yu J., et al., (2010), López R. , et al., (2011), Morales-Flores N., et al., (2011)). The optical properties recorded for the films, UV-Vis spectra, low transmittance, and interference effects and therefore a relatively low transparency, prevents the penetration of UV rays that could activate the structure of the composites.

No doubt there are more fundamental factors that explain the possible mechanisms of reactions in the film-solution interface, where the generation of hydroxyl ions (OH^-) from the humid environment or H_2O with radiation and of course the response from TiO_2/ZnO to UV radiation, where the electron-hole pairs are generated, $ZnO \rightarrow ZnO\ (e^- + h^+)$, assuming the surface of the composite, and h^+ when migrating to the semiconductor surface, or to the active sites available, will react with the OH^- ions, resulting in hydroxyl ions excited •OH, which can react and attack the MO molecule and with it the possible production of MO intermediate compounds or other less aggressive and more treatable derivatives; on the other hand, the e^- can be trapped by dissolved oxygen and produce the super oxide O^{2-}, that is, $e^- + O_2 \rightarrow O^{2-}$ (Yu J., et al., (2010)) or also the vacancies of oxygen that operate as photoelectron traps; the water molecule H_2O adsorbed turns out to be very important in the possible reactions. Therefore, the possible reactions that take place in the film-solution interface, between grain boundaries and/or charge transfer between the TiO_2/ZnO components can be explained (Yu J., et al., (2010), Lara A. del Angel (2014)).

Luminescence properties

To characterize the emission spectra (PL) of the samples in the range 300-500 nm recorded at room temperature, they were irradiated with ultraviolet light of wavelength 325 nm (3,81 eV). Thus, the emission spectra of the TiO_2/ZnO composites (TZi) shown Graph 12, were recorded.

For the TZ0 sample *a)*, the intense broadband was presented at 374,77 nm (3,308 eV) and at 389,79 nm (3,18 eV) of intensity 756,60 accounts, besides the bands in 2,82, 2,74 and 2,64 eV, the latter of greater relative intensity.

In the spectrum of TZ1 sample *b)*, a wide band with peaks in 371,69 nm (3,336 eV) and the highest peak at 381,73 nm (3,248 eV) with intensity 374,55 counts, were resolved; the peaks are resolved in 2,948, 2,863, 2,762 eV (of greater relative intensity), 2,649 eV (with structure and wide) and in 2,577 eV. For the sample TZ3 with three layers of ZnO or spectrum *c)*, there are bands in 3,246 eV (382 nm) (which are decreasing in intensity), 3,155 eV (395 nm), 2,743 eV (wide band) and that of relative intensity greater in 2,649 eV (469 nm) bands that remain. The signal in the sample TZ5 or *d)*, the band in 3,229 eV (384 nm) that decreases its intensity with respect to the previous samples, signal in 2,903 eV (that persists) (427 nm) and the broad band with structure in 2,643 eV (469 nm) that still resolves. For metal oxides such as TiO_2 or ZnO, both components of the composites, the phenomenon of photoluminescence is explained based on different types of defects, among which are the different kinds of oxygen vacancies, Ti or Zn or positions interstitial Oi, Ti, Zn, or others (Lin B., et al., (2001), Liu H., et al., (2013), Guo QX, et al., (2008), Korotcenkov G.B., et al., (2010)), which is presented in thin films of TiO_2 or other structures (Yu J., et al., (2000), Fusi M., et al., (2013), Lei Y., et al., (2001), Cruz-González N., et al., (2013)). Methods of preparing systems, precursors and heat treatment are related to structural and intrinsic defects (Lin B., et al., (2001), Yu J., et al., (2000), Nada A., et. al., (2014), Lim J., et al., (2004)).

In general, the transitions that define the photoluminescence spectra are associated to oxygen vacancies, as well as to different types of defects in the samples, which for the case of the TZ0 sample *a)*, the value of 3,308 eV would be associated with electronic transitions between the conduction band (CB) and the valence band (VB) of the TiO_2, while the 3,336 eV of TZ1 or *b)*, can be associated with the ZnO equivalent transitions of the TiO_2/ZnO system with a layer of zinc oxide; the transitions in 3,18 eV and in 3,248 eV can be associated with transitions close to the absorption edges of the respective components.

ECORFAN® All rights reserved.

The transitions that have been identified in the spectra of the samples are generated from superficial vacancies or other types of defects (donor centers) to near or deep states at the base of the valence band (acceptor states) (Tripathi A., et. al., (2014), Lei Y., et al., (2001)). Due to the behavior of the bands in the photoluminescence spectra, which decrease in intensity or are modified, the ZnO deposit process affects the population of donor levels participating in the transitions given by phonon mechanisms or recombination of free excitons (Lin B., et al., (2001), Guo Q.X., et al., (2008), Korotcenkov G.B., et al., (2010), El Hichou A., et al., (2004) and refs. there in, De- Wei M., et al., (2003)). Oxygen vacancies and hydroxyl groups play an important role in slowing the recombination of photogenerated electron-hole pairs, which would manifest in the photocatalytic efficiency by degrading the MO of the aqueous solution (Liu G., et al., (2009), Nada A., et al., (2014), Maldonado A., et al., (2010)).

The well-defined band in the UV zone, as well as the intensity present in the emission spectra that decreases with the surface modifications of the TiO_2/ZnO composites, these systems have the possibility of being used as dosimeters in the UV region, over all the TZ0 films and those of TZ1 with a layer of ZnO. Visible transitions are maintained for both the TZ0, and the TZ1 sample corresponding to a ZnO layer (Lin B., Fu Z., Jia Y., (2001)).

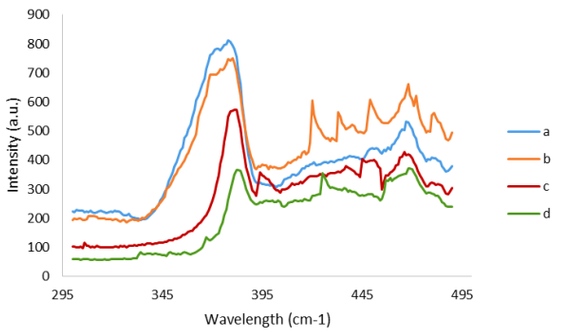

Graphic 12 Photoluminescence of the series of TZi composites, a), b), c) and d) for the four samples

Conclusions

TiO_2/ZnO (TZi) composites were synthesized in thin film with the use of sol-gel and repeated immersion. The sols were generated from titanium (IV) oxyacetylacetonate and zinc acetate, respectively. The technique was implemented in the laboratory. The film thickness at five layers of TiO_2 (TZ0) resulted around 87 nm on average, thickness that increases with the number of layers of ZnO (133 nm).

The five-layer structure of the TiO_2 substrate resulted amorphous (XRD), but the TZi composites were polycrystalline, especially those with three and five layers of ZnO. With Raman spectroscopy, the phases of anatase (TiO_2) mainly and the wurtzite phase of ZnO were confirmed separately. The morphology and composition of the composites was determined by scanning microscopy (SEM) and by electron dispersion spectroscopy (EDS) the Ti, O and Zn components of composites were identified. Porous films were recorded in the TZi composites. The topography and recorded roughness parameters (AFM) show a uniform grain distribution (17.7 nm) which is consistent with the crystal size (XRD), itself that varies with the number of ZnO layers.

By UV-Vis spectroscopy, films with low transmittance and interference effects were recorded, with absorption board around 375-399 nm. The band gap of the semiconductor *Eg* was estimated between 3.00 and 2.93 eV for the pure TiO_2 film and that with a ZnO layer, respectively.

For composites with three and five layers of ZnO the values of *Eg* are not consistent with the previous data.

The surface ionic components Ti^{4+}, Zn^{2+}, the different species of the orbital O1s (O^{2-}, hydroxyl OH^-, among others), the carbon orbital, C1s (C-C or C-H, or others), as well as their binding energies were determined by XPS. The recorded values confirm the formation of TiO_2 and ZnO, among others possible intermediate compounds, which reflect the experimental conditions.

The photodegradation of the methyl orange solution (504 nm band) (UV-Vis), by the TZi composites, irradiated with UV-Vis, resulted in the order (Graphs 10 and 11): TZ5 sample > TZ0 sample > TZ3 with three layers > TZ0 one layer of ZnO. There is no clear order that reflects the expected behaviors according to the growth conditions of the prepared films. In order to have adequate catalysts, it would be necessary to optimize them by varying experimental conditions.

ISSN-On line: 2414-4924
ECORFAN® All rights reserved.

The emission spectra of the TZi composites (Graph 12), presented a wide emission band in the well-defined UV region and variable bands in the intermediate and visible regions. The TZ0 sample presented the UV emission of greater intensity, whereas in the TZ1 film with a layer of ZnO, the intensity decreased with respect to the first one; for three and five layers of ZnO the intensity decreases.

The emission band in the UV of the TiO_2/ZnO composites would allow these devices to be applied as dosimeters, especially the thinnest ones and photodegradation in catalysis heterogeneous.

Acknowledgments

SIP-IPN Research Proyects 20171063 and 20181555, SEM, X-ray and XPS to NCNM-IPN, to Gabriela Rueda, to Natzin Tirado for editing this paper and to Ing. Omar Rios Berny by recording the photodegradation and photoluminescence spectra.

References

Castrejón-Sánchez V.H., Camps E. Camacho-López M., (2014). Quantification of phase content in TiO_2-thin films by Raman spectroscopy. Superficie y Vacío 27(3), 88-92.

Chae Y.K., Won Park J., Mori S., Suzuki M., (2013). Photocatalytic effects of plasma-heated TiO_{2-x} particles under visible light irradiation. Korean J. Chem. Eng. 30(1), 62-63.

Cruz-González N., Fernández-Muñoz J.L., Zapata-Torres M., (2013). Efecto del gas utilizado en el tratamiento térmico y la impurificación con Eu en las propiedades estructurales de nanofibras de TiO_2 depositadas por electrohilado. Superficie y Vacío 29 (3), 111-116.

Damen T.C., Porto S.P.S., Tell B., (1966). Raman Effect in Zinc Oxide. Physical Rev. 142 (2), 570-574.

De-Wei M., Zhi-Zhen Y., Jing-Yun H., Bing-Hui Z., Shou-Ke W., Hue-Hao S., Zhan-Guo W., (2003). Structural and optical characterization of $Zn_{1-x}Cd_xO$ thin films deposited by dc reactive magnetron sputtering. Chin. Phys. Lett. 20 (6), 942-943.

El Hichou A., Addou M., Bougrine A., Dounia R., Ebothé J., Troyon M., Amrani M., (2004). Cathodoluminescence properties of undoped and Al-doped ZnO thin films deposited on glass substrate by spray pyrolysis. Mat. Chem. and Phys. 83, 43-47.

Fusi M., Maccallini E., Caruso T., Casari C.S., Bassi A.L., Bottani C.E., Rudolf P., Prince K.C., Agostini R.G., (2011). Surface electronic and structural properties of nanostructured titanium oxide grown by pulsed laser deposition. Surface Science 605, 333-340.

Guo Q.X., Mitsuishi Y., Tanaka T., Nishio M., Ogawa H., (2008). Microfabrication of ZnO on a PTFE templete patterned by using synchrotron. J. Korean Phys. Soc. Vol. 53, 5, 2796-2799.

Giannakopoulou T., Todorova N., Giannouri M., Jiaguo Yu, Trapalis C., (2014). Optical and photocatalytic properties of composite TiO_2/ZnO thin films. Catal. Today 230, 174-180.

Hermann J.M., (1995). Environmental applications of semiconductors photocatalysis. Chemical Rev. 95, 69-96.

Hermann J.M., Hoffmann M.P., Martin S.T., Choi W., Bahnemann D.W., (1999). Heterogeneous photocatalysis: fundamentals and applications to the removal of various types of aqueous pollutants. Catalysis Today 53, 115-129.

Jongnavakit P., Amornpitoksuk P., Suwanboon S., Ratana T., (2012). Surface and photocatalytic properties of ZnO thin film prepared by sol-gel method. Thin Solid Films 520, 5561-5567.

Korotcenkov G.B., Cho B.K., Nazarov M., Noh Do Y., Kolesnikova E.V., (2010). Cathodoluminiscence studies of un-doped and (Cu, Fe, and Co)-doped tin dioxide films deposited by spray pyrolysis. Current Appl. Phys. 10, 1123-1131.

Lara del Ángel A., (2014). Espectroscopia Raman de películas de GaN y ZnO para aplicaciones fotovoltaicas. Tesis Maestría.

Lei Y., Zhang L.D., Meng G.W., Li G.H., Zhang X.Y., Liang C.H., Chen W. and Wang S.X., (2001). Preparation and photoluminescence of highly ordered TiO_2 nanowire arrays. Am. Inst. of Phys., DOI: 10.1063/1.1350959.

Lim J., Shin K., Kim H.O., Lee C., (2004). Photoluminescence studies of ZnO thin films grown by atomic layer epitaxy. 109, 181-185.

ECORFAN® All rights reserved.

Lin B., Fu Z., Jia Y., (2001). Green luminescent center in undoped zinc oxide films deposited on silicon substrates. Appl. Phys. Letters 79 (7), 943-945.

Liu F., Yan X., Chen X., Tian L., Xia Q., (2016). Mesoporous TiO_2 nanoparticles terminated with carbonate-like groups: Amorphous/crystalline structure and visible-light photocatalytic activity. Catalysis Today 264, 243-249.

Liu G., Li G., Qiu X., Li L., (2009). Synthesis of ZnO/titanate nanocomposites with highly photocatalytic activity under visible light irradiation. J. of Alloys and Compounds 481, 492-497.

Liu H., Wang J., Fan X.M., Zhang F.Z., Liu H.R., Dai J., Xiang F.M., (2013). Synthesis of CuO_2/T-ZnO_w nanocompound and characterization of its photocatalytic activity and stability property under UV irradiation. Materials Science and Engineering B 178, 158-166.

López R., Díaz T., Rosendo E., García G., Coyopol A., Juárez H., (2011). Propiedades fotoluminiscentes de películas ZnO: A-SiOx obtenidas por la técnica CVD asistido por filamento caliente. Rev. Latin. de Met. y Materiales 31 (1), 59-63.

Luna, A.L., Valenzuela M.A., Colbeau-Justin C., Vázaquez P., Rodríguez J.L., Avendaño J.R., Alfaro S., Tirado S., Garduño A., De la Rosa J.M., (2016). Photocatalytic degradation of galic acid of CuO-TiO_2 composites under UV/Vis LEDs irradiation. Applied Catalysis A: General 521, 140-148.

Luna, A.L., Dragoe E., Wang K., Beaunier P., Kowalska E., Ohtani B., Bahena Uribe D., Valenzuela M.A., Remita H., Colbeau-Justin C., (2017). Photocatalytic Hydrogen Evolution Using Ni-Pd/TiO_2: Correlation of Light Absorption, Charge-Carrier Dynamics, and Quantum Efficiency. J. Phys. Chem. C 121 (26), 14302-14311.

Maldonado A., Mallén-Hernández S.A., Tirado-Guerra S. and Olvera M. de la L., (2010). Titanium dioxide thin films deposited by the sol-gel technique starting from titanium oxy-acetyl acetonate: gas sensing and photocatalyst applications. Phys. Status Solidi C 7, No. 9, 2316-2320.

Martínez A.I., Acosta D.R., Cedillo G., (2005). Effect of SnO2 on the photocatalytical properties of TiO2 films. Thin Solid Films 490, 118- 123.

Morales-Flores N., Pal U., Sánchez Mora E., (2011). Photocatalytic behavior of ZnOand Pt-incorporated ZnO nanoparticles in phenol degradation. Applied Catalysis A: General 394, 269-275.

Nada A., Moustafa Y., Hamdy A., El-Wahab S.A., Yahea D., (2014). Synthesis and photocatalytic activity of single crystal titanate-Part-1. Chem. And Mats. Res. 6 (10), 40-49.

Ochoa Y., Ortegón., Vargas M., Rodríguez-Páez J.E., (2009). Síntesis de TiO_2, fase anatasa, por el método Pechini. Rev. Lat. De Metal. Y Mater. S1 (3), 931-937.

Pérez-Álvarez J., Escobar-Alarcón L., Camps E., Romero S., Fernández-Valverde S.M., Jiménez-Becerril J., (2007). Caracterización de bicapas TiO_2/son_2 depositadas por ablación láser para fotocatálisis. Superficie y Vacío 20 (2), 12-16.

Ramírez-Ortega D., Meléndez A.M., Acevedo-Peña P., González I., Arroyo R., (2014). Semiconducting properties of ZnO/TiO_2 composites by electrochemical measurements and their relationship with photocatalytic activity. Electrochimica Acta 140, 541-549.

Tripathi A., Misra K.P., Shukla R.K., (2014). UV enhancement in polycrystalline Ag-doped ZnO films deposited by de sol-gel method. Journal of Luminescence 149, 361-368.

Yu J., Zhao X., Zhao Q., (2000). Effect of surface structure on photocatalytic activity of TiO_2 thin films prepared by sol-gel method. Thin Solid Films 379, 7-14.

ISSN-On line: 2414-4924
ECORFAN® All rights reserved.